Copper oxide / peroxydisulfate system for urban wastewater disinfection: Performances, reactive species, and antibiotic resistance genes removal

Chan Li[1], Vincent Goetz[2] and Serge Chiron[1*]

[1]UMR5151 HydroSciences Montpellier, University of Montpellier, IRD, 15 Ave Charles Flahault 34093 Montpellier cedex 5, France

[2]PROMES-CNRS UPR 8521, PROcess Material and Solar Energy, Rambla de la Thermodynamique, 66100 Perpignan, France

*Corresponding author: Tel: + 33 - 411759415; Fax: + 33 - 411759414; e-mail address: serge.chiron@umontpellier.fr

Abstract

In this study, copper oxide (CuO) catalyzed peroxydisulfate (PDS) system was investigated for the inactivation of a broad range of pathogenic microorganisms from urban wastewater. Complete inactivation of *Escherichia coli*, *Enterococcus*, *F-specific RNA bacteriophages* from secondary treated wastewater was achieved after a short time (15-30 min) treatment with CuO (10 g/L) / PDS (1 mM) system, but *spores of sulfite-reducing bacteria* took 120 min. No bacterial regrowth occurred during storage after treatment. Significant reduction of the pathogens was explained by the generation of the highly selective Cu(III) oxidant, as the predominant reactive species, which could quickly oxidize guanine through a one-electron oxidation pathway. Additionally, the potential of the CuO (10 g/L) / PDS (1 mM) system to inactivate antibiotic-resistant bacteria and antibiotic resistance genes (ARB&Gs) was explored. Sulfamethoxazole-resistant *E. coli* was used as the model ARB and a 3.2 log of reduction was observed after 10 min of treatment. A considerable reduction (0.7-2.3 log) of selected ARGs including blaTEM, qnrS, emrB, sul1, and genes related to the dissemination of antibiotic resistance, including the Class 1 integron-integrase (intI1), and the insertion sequence (IS613) was achieved after 60 min treatment. All these findings indicated the promising applicability of the CuO/PDS system as a disinfection technology for wastewater reuse in agriculture.

Keywords: Urban wastewater; disinfection; CuO; antibiotic resistance genes; cupryl ion.

1. Introduction

Wastewater (WW) reuse in agriculture is a growing practice worldwide to alleviate the demand pressure on freshwater sources, moderate water pollution, and to reduce the use of additional fertilizers resulting in savings for the environment, wastewater treatment, and farmers (Akhoundi and Nazif, 2018; Hong et al., 2013). WW after secondary or tertiary treatments is usually considered, but people in some poor and developing countries have to reuse untreated raw wastewater because of the lack of provisions by the authorities (Aslani et al., 2014). Whatever the resource, this latter contains various microbial contaminants, mainly including pathogenic bacteria, viruses, and protozoa. These biological contaminants have posed potential risks in spreading foodborne diseases and threaten public health when reclaimed WW has been used for irrigation (Hong et al., 2018; Hwangbo et al., 2019). In addition, WW also is seen as the reservoir and environmental supplier of antibiotics resistance, where antibiotic-resistance genes (ARGs), acquired by different bacteria species via genes transfer or extracellular uptake (Karkman et al., 2018; Pazda et al., 2019) intensively spread. Although antibiotic-resistant bacteria and antibiotic resistance genes (ARB&Gs) are not currently included in any international regulation, they have been recognized as one of the major challenges for human health by the World Health Organization (WHO, 2015). To meet the minimum quality requirements for the safe reuse of WW in agricultural irrigation, inactivating a broad range of pathogenic microorganisms and limiting the spread of antibiotics resistance (ARB&Gs) by effective disinfection technologies are highly recommended.

The most commonly used disinfection technologies are chlorination, UV-C treatment, and peracetic acid. Chlorine is still the most widely used disinfectant due to its low cost and high efficiency for the inactivation of microbes. However, it is not efficient for cryptosporidium removal together with the well-known problem of unhealthy disinfection by-products generation (Hashemi et al., 2013; Vasilyak, 2021). UV irradiation requires extensive secondary

58 treatment and sand filtration to reach a recommended water transmittance value over 50% and
59 is not adapted to open treatment systems (e.g., lagooning or constructed wetlands) where green
60 colored microscopic algae can grow (Hashemi et al., 2013). Besides, potential bacterial
61 regrowth problems during treated WW storage for UV doses below 40-60 mJ/cm^2 have been
62 reported (Hashemi et al., 2013; Vasilyak, 2021). Peracetic acid has shown poor effectiveness in
63 removing enteric viruses, and potential microbial regrowth (Gehr et al., 2003; Kitis, 2004).
64 Homogeneous advanced oxidation processes (AOPs) employing hydrogen peroxide (H_2O_2) and
65 persulfate (PDS) and relying on hydroxyl and/or sulfate radical (·OH and $SO_4^{\cdot-}$) production
66 have obtained increasing attention and have shown high disinfection capacity but can only be
67 an interesting option when organic micropollutants have to be simultaneously removed due to
68 the high operational and maintenance costs of those processes (Chen et al., 2021). To overcome
69 the disadvantages of the traditional homogeneous Fenton reaction and AOPs such as the narrow
70 pH range of implementation and the production of a large amount of iron-containing sludge
71 (Chen et al., 2021), heterogeneous Fenton-like oxidation processes (HFOPs) make use of
72 recyclable solid catalysts, such as iron oxides (de la Obra Jiménez et al., 2020; Xia et al., 2017),
73 copper oxide (Cho et al., 2020; Zhang et al., 2014), metal-organic frameworks (MOFs, Lu et
74 al., 2021), layered double hydroxides (LDHs, de Melo Costa-Serge et al., 2021), developed
75 rapidly in recent years. It should be noted that disinfection processes are widely applied as the
76 last barrier in the WW reclamation train after carbon and nutrients removals. However, in
77 irrigation application, what is needed is a disinfection method that can work in presence of high
78 contents of dissolved organic matter and nutrients because both are valuable agronomic
79 parameters to be preserved (Jaramillo and Restrepo, 2017). Organic matter is a well-known
80 hydroxyl and sulfate radical scavenger, limiting the efficiency of those processes (Chen et al.,
81 2021). However, HFOPs still mostly rely on radical generation. This work contemplated the
82 possibility to implement a HFOP relying on more selective reactive species than sulfate and

hydroxyl radicals, which might work in organic-rich WW.

For this purpose, this work benefited from recent results of our research group, which have shown that the copper oxide (CuO) / peroxydisulfate (PDS) system is a good generator of the highly selective cuprous (Cu(I)) and cupryl (Cu(III)) as well as singlet oxygen ($^1O_2$) species and could efficiently eliminate phenol and a mixture of antibiotics from WW (Li et al., 2021). As Cu(I), Cu(III), and $^1O_2$ are well identified as excellent biocidal species in the literature (García-Fresnadillo, 2018; Kim et al., 2015), good disinfection performance of the CuO/PDS system was anticipated, but to our knowledge, the study of CuO/PDS on urban wastewater disinfection has not been reported yet. Consequently, the main objective of this work was to demonstrate the performances of this system in inactivating a broad range of pathogenic microorganisms. Specific objectives included i) a comparison of the disinfection capacity in raw and secondary-treated WW, ii) the identification of the predominant reactive species and iii) the evaluation of the abundance reduction of selected ARB&Gs.

2. Material and Methods

2.1 Chemicals

Micrometer copper oxide particles (CuO, 44 µm particle size on average) were purchased from Alfa Aesar (Kandel, Germany). Guanine, thymine, adenosine, L-tyrosine, ranitidine, ranitidine N-oxide, ranitidine sulfoxide, sodium hydroxide (NaOH), sodium thiosulfate (NaS_2O_3), sulfamethoxazole (SMX), and EDTA were purchased from Sigma-Aldrich (Saint Quentin Fallavier, France). Potassium persulfate ($K_2S_2O_8$), sodium hypochlorite (NaOCl), formic acid, ammonium acetate, Chromocult coliforms agar, Slanetz Bartley agar, and tris(hydroxymethyl)aminomethane (Tris) were purchased from Merck KGaA (Germany). Acetonitrile (HPLC grade) and methanol (HPLC grade) were purchased from Carlo Erba reagents (France). All solutions were prepared with ultrapure water obtained from a Milli-Q

Plus system (Millipore, Bedford, MA). Stock solutions of adenosine (100 mg/L), thymine (100 mg/L), ranitidine (100 mg/L), L-tyrosine (100 mg/L) and PDS (100 mM) were prepared in ultrapure water. Guanine stock solution (500 mg/L) was prepared in 10% NaOH solution due to its poor water solubility at neutral pH.

2.2 Pathogens inactivation

Wastewater disinfection. Influents and effluents were collected at the inlet and the outlet of a conventional activated sludge wastewater treatment plant (WWTP, 20,000 equivalent inhabitants). The major physico-chemical properties of collected influent and effluent samples are shown in Table 1. The main differences when switching from influent to effluent were the decrease of total suspended solids (TSS, 14 folds decrease) and chemical oxygen demand (COD, 20 folds decrease) values, and the simultaneous decrease of NH_4^+ and increase of NO_3^- ions caused by nitrification. Before being subjected to treatment, the wastewater samples were firstly filtered through a 200 µm sieve to remove the biggest suspended solid particles. This effluent was named pre-filtered effluent along the manuscript. The filtration had no significant influence on the number of microorganisms present in WW. In other words, the microbial load did not change before and after filtration.

To the tests devoted on the efficiency of the CuO/PDS system, chlorine considered as the reference for disinfection operation and thermal activation of persulfate as the $SO_4^{\cdot-}$ radical based process were also carried out. Before the use of CuO, this latter was rinsed around10 times with tap water in a 1-liter bottle to remove the suspended particles until almost all CuO could settle down within 1 min. The washed CuO was dried in an oven (50 °C) for further use. CuO (10 g/L), PDS (1 mM), CuO (10 g/L)/PDS (1mM), and free chlorine (2.6 mg/L) were added to the pre-filtered effluent, separately. One liter WW bottles with or without PDS (1mM) addition were immersed in a water bath (15 L) at 70 °C to ensure the full activation of PDS into

sulfate radicals. CuO particles were easily removed by spontaneous decantation, and analyses were performed on the supernatant. Samples (500 mL) were collected in sterilized plastic bottles at defined time intervals of treatment. Excess EDTA (5 mM) and/or sodium thiosulfate (5 mM) were added immediately for released Cu^{2+} complexation and excess PDS removal, respectively. Samples were stored at 4 °C and pathogens analysis was conducted less than 24 h after sample collection. Potential bacterial regrowth was evaluated by analyzing treated effluent samples collected at various time intervals after 24 and 48 h of storage in the ambient environment. For influent, the procedures are the same as the effluent disinfection experiment using CuO (10 g/L) and PDS at different concentration levels (i.e., 1, 2.5, and 10 mM).

Enumeration of pathogens. The NF EN ISO 9308-3 and NF EN ISO 7899-1 standard protocols were used to enumerate *Escherichia coli (E. Coli)* and *Enterococcus* respectively. These methods are based on the culture of the bacteria in a liquid medium and the determination of the most probable number (MPN) according to the level of dilution. The NF EN 26461-2 standard protocol was used to enumerate the colony-forming unit (CFU) of *spores of sulfite-reducing bacteria* after filtration and cultivation on a specific agar solid medium. *F-specific RNA bacteriophages* were measured according to the ISO 10705-1 method. This method allows for a count on the agar medium of plaque-forming unit (PFU), corresponding to the number of viruses. All results are presented as an average of two experiments.

Analysis of Cu. Cu was analyzed by inductively coupled plasma - optical emission spectrometry (ICP-OES) using an iCap Duo 7400 spectrometer (Thermo Fischer Scientific, Les Ulis, France) using the axial mode of detection at wavelength $\lambda = 324.754$ nm.

Analysis of PDS. The analytical method for PDS is reported in Li et al., (2021).

Analysis of trihalomethanes (THMs). Chloroform (CFL), dichloromonobromomethane (DCB), monochlorodibromomethane (MCB), and bromoform (BRF) were determined following the EPA 551A method.

158

159 **2.3 Identification of reactive species**

160 *Experimental procedures.* Batch experiments were conducted in 100 mL glass serum bottles
161 under continuous shaking at 60 rpm using a roller mixer (STUART® SRT9D, UK) and 200
162 mM Tris buffer adjusted to pH 7 with HCl. Typically, target compounds (guanine, thymine,
163 adenosine, ranitidine, L-tyrosine), CuO, and PDS were sequentially added into the bottles to
164 reach initial concentrations of 20 mg/L, 10 g/L, and 1 mM, respectively. Sample aliquots (5 mL)
165 were taken at predetermined times and filtered through 0.45 μm cellulose membrane filters, and
166 then stored in 6 mL glass tubes at 4 °C before analysis. Control experiments in presence of CuO
167 or PDS alone were also performed under the same experimental conditions. 100 mM of
168 methanol was added to the CuO/PDS system as a hydroxyl and sulfate radical scavenger.
169 *Analytical methods.* Degradation kinetics of selected compounds were followed by liquid
170 chromatography (LC) with a diode-array detector (DAD) and using an Agilent ZORBAX
171 Eclipse XDB C18 column (150 × 3 mm i.d., 3.5 μm particle size). The separation and detection
172 conditions are shown in Table S2. Transformation products (TPs) of guanine, L-tyrosine, and
173 ranitidine were identified by LC-high resolution-mass spectrometry (LC-HRMS) composed of
174 a Dionex Ultimate 3000 liquid chromatograph equipped with an electrospray source operated
175 in the positive ionization mode and an Exactive Orbitrap mass spectrometer (ThermoFisher
176 Scientific, Les Ulis, France) operated in full scan mode (mass range m/z 50-900) and using the
177 reverse phase PFPP (pentafluorophenylpropyl) analytical column (100 mm × 2.1 mm; 3 μm
178 particle size). LC gradient consisting of Milli-Q water with 1% ACN and 0.1% formic acid
179 (solvent A) and ACN with 1% Milli-Q water and 0.1% formic acid (solvent B) was as follow:
180 0-1.5 min, 98% A; 11.25 min, 55% A; 12.75 min, 30% A; 13.0-20 min, 98% A. The flow rate
181 was set at 0.3 mL/min. The energy collisional dissociation was set to 20 eV and a drying gas
182 temperature of 300 °C was used. TPs of guanine, L-tyrosine, and ranitidine were identified

following a suspect screening workflow in LC-HRMS. The databases were made up of a list of possible TPs with their molecular formula and exact mass (Table S3–S5) collected from the literature.

2.4 Antibiotic-resistant bacteria and antibiotic resistance genes (ARB&Gs)

Antibiotic-resistant bacteria. SMX-resistant *E. coli* and *Enterococcus* were quantified before and after treatment to examine the ARBs inactivation performances. Considering the observed minimum inhibitory concentration (MIC) (Iakovides et al., 2019; CLSI, 2020), 516 mg/L of SMX was added to the Chromocult coliform agar (*E. coli*) and Slanetz Bartley agar (*Enterococcus*), respectively. After membrane filtration and cultivation, the colony-forming unit (CFU) of SMX-resistant and total *E. coli* and *Enterococcus* on the agar was counted. The prevalence of SMX-resistant *E. coli* and SMX-resistant *Enterococcus* were calculated as the ratio between the CFU/100 mL observed on the antibiotic supplemented culture medium and the CFU/100 mL observed on the same medium without antibiotic ($prevalence\ (\%) = \frac{CFU\ 100\ mL^{-1} medium\ with\ SMX}{CFU\ 100\ mL^{-1} medium\ without\ SMX} \times 100$). All results are presented as an average of two experiments.

Antibiotic resistance genes. 100 mL of pre-filtered effluents collected before and after treatment were filtered on 0.22 µm polyethersulfone filters (Millipore, France). DNA extraction was performed with the filters by following the specific protocols of the Qiagen DNeasy® PowerWater® Kit (Qiagen GmbH, Hilden, Germany). DNA purity and concentrations were estimated by spectrophotometry (Infinite NanoQuant M200, Tecan, Austria). The extracted DNA was stored at -20 °C before analysis. Four ARGs and two genes linked to the dissemination of antibiotic resistance were quantified by droplet digital PCR (ddPCR) using EvaGreen chemistry: qnrS (reduced susceptibility to fluoroquinolone); sul1 (resistance to sulfonamides); blaTEM (resistance to β-lactams), ermB (resistance to macrolide), intI1

encoding the integrase of Class I integron-integrase used as a proxy for the potential capacity of the bacterial community to disseminate resistance (Iakovides et al., 2019), and IS613 selected as one representative of insertion sequences in DNA transposons (Babakhani and Oloomi, 2018). The 16S rRNA gene, as an indicator of total bacteria, was quantified by quantitative PCR (qPCR) using EvaGreen chemistry. The amplification and quantification processes were conducted as the following protocol: 2 min at 95 °C for pre-incubation of the DNA template, followed by 40 cycles at 95 °C for 15 s for denaturation and 60 s for annealing (at specific annealing temperature) and amplification. Primers' information and annealing temperature are listed in Table S3. Specificity of amplification was validated both by melting curve analyses and by checking the size of the amplicons on 2100 Bioanalyzer (Agilent, Waldbronn, Germany). All results are presented as an average of three replicates.

3. Results and discussion

3.1 Inactivation performances of pathogens

3.1.1 Effluent

E. coli is commonly used as an organism indicator to indicate the fecal contamination level (Odonkor and Ampofo, 2013). However, the thin cell wall of Gram-negative *E. coli* makes it poorly resistant to many types of disinfectants. Thus, the Gram-positive *Enterococcus* with a relatively thick and dense layer composed cell wall was adopted as a more resistant and reliable indicator of fecal pollution (Núñez-Salas et al., 2021). Considering that bacterial indicators are unable to indicate the occurring level of viral pathogens (Dias et al., 2018), *F-specific RNA bacteriophages* was used as the appropriate pathogenic viral indicator. *Spores of sulfite-reducing bacteria* were selected as an indicator of protozoa. All these indicators are also included in the EU Regulation 2020/741 of the European Parliament and of the Council of 25 May 2020 on minimum requirements for water reuse" (EU, 2020) to evaluate performances of

disinfection technologies.

The initial abundances in secondary-treated effluent samples before treatment were 4.6 ± 0.1 log_{10} MPN/100 mL of *E. coli*, 3.5 ± 0.2 log_{10} MPN/100 mL of *Enterococcus*, 2.7 ± 0.2 log_{10} PFU/100 mL of *F-specific RNA bacteriophages*, and 3.2 ± 0.1 log_{10} CFU/100 mL of *spores of sulfite-reducing bacteria* and are comparable to the values found in the literature (Haramoto et al., 2015; Mandilara et al., 2006). The inactivation performances on four pathogenic indicators by PDS alone, CuO alone, CuO/PDS, thermally activated PDS system ($SO_4^{\cdot-}$), and chlorination (Cl_2) are shown from Fig. 1 (a) to Fig. 1 (d). No effective inactivation performance of any indicator was observed by using PDS alone. As shown in Fig. 1 (a)-(b), significant reduction of *E. coli* (> 3.0 log) and *Enterococcus* (> 1.7 log) was observed for the other three systems after a short treatment time (15 - 30 min) and no cultivable cells were detected after that. This result is comparable to UV-C irradiation, which can usually inactivate 2-4 log of *E. coli* (Collivignarelli et al., 2018). All the disinfection systems except PDS alone efficiently removed *F-specific RNA bacteriophages* (Fig.1 (c)). However, this result was not strong enough to fully demonstrate the effective inactivation activity of these systems for viral pathogens because the initial concentration of *F-specific RNA bacteriophages* (2.7 ± 0.2 log_{10} PFU/100 mL) was too low and close to the detection limit (2 log_{10} PFU/100 mL). Significant reduction (> 1.5 log) of *spores of sulfite-reducing bacteria* was only obtained with Cl_2 and CuO/PDS systems after 15 min and 120 min treatment time, respectively (Fig.1 (d)). As a whole, CuO/PDS system took a longer time than chlorination for the removal of targeted indicators. However, the CuO/PDS system did not imply the generation of unhealthy trihalomethanes (THMs) as shown in Table 2. The lack of THMs production held also true for the sulfate radical-based treatment.

Interestingly, CuO alone demonstrated good disinfection performances for all pathogenic indicators. The released cupric ion (Cu(II)) was suggested to be responsible for the antimicrobial activity of CuO (Dizaj et al., 2014; Suleiman et al., 2015), which is mainly due

to the cytotoxicity of cellularly generated cuprous ion (Cu(I)) (Kim et al., 2015). In this study, the Cu(II) released from CuO was up to 315 ± 15 µg/L, so that the antimicrobial level was reached. It is reported that Cu (II) can effectively inactivate bacteria, yeast cells and algae, but has minor effects on virus inactivation (Kim et al., 2015). However, in combination with PDS, the biocidal activity was significantly improved due to an acceleration in the generation of high-valent copper species such as the virucide Cu(III) ions as detailed in section 3.2. For a better understanding of the role of dissolved Cu in disinfection processes, Cu was measured in the water phase together with the consumption of PDS at different times (Fig.2 (a) and (b)). A positive correlation between Cu leaching and PDS consumption was observed. At the beginning of the reaction, the fast consumption of PDS was associated with a strong Cu release up to 848 ± 42 µg/L. After 60 min treatment, PDS consumption dramatically slowed down and Cu release decreased down to 392 ± 20 µg/L. The mechanisms of PDS activation by CuO might account for this specific behavior. At neutral pH, the CuO surface is positively charged as pHpzc was 8-9 have been reported (Ghulam et al., 2013) and PDS is an anion calling for strong electrostatic interactions. The first step involves an electrostatic interaction of PDS on the CuO surface followed by PDS decomposition into superoxide radical anion (Li et al., 2021). As the reaction proceeds, active sites on CuO might become occupied by waterborne molecules or even by Cu^{2+} limiting PDS activation and Cu^{2+} leaching. As PDS was found not to be the limiting factor in disinfection, further studies using lower PDS doses are needed to reduce Cu(II) leaching.

For bacterial regrowth study, treated samples collected at various time intervals: 5, 10, and 30 min were stored under ambient conditions, and the occurrence and viability of *E. coli* and *Enterococcus* in treated WW after 24 h and 48 h of storage was evaluated. Complete inactivation of *E. coli* and *Enterococcus* was achieved after 30 min of treatment, no regrowth of bacteria in the treated WW was observed during the storage time while incomplete inactivation was observed after 5 and 10 min of treatment. CuO/PDS system achieved a

283 reduction of 1.0 log and 2.3 log of *E. coli* and 0.3 log and 1.5 log of *Enterococcus*, respectively
284 (Fig. 3). Still no regrowth of *E. coli* and *Enterococcus* in treated WW samples was observed
285 after 24 h and 48 h of storage at ambient conditions, which might indicate that the possibility
286 for damaged DNA repair was restricted in the CuO/PDS system.
287
288 3.1.2 Influent
289 The inefficiency of raw WW disinfection has often been attributed to chemical/radical
290 disinfectant inhibition in presence of the high concentrations of inorganic and organic matters.
291 Sánchez-Ruiz et al., (1995) used peracetic acid to inactivate total coliforms in raw WW but
292 great variability in inactivation efficiency under different pH conditions and bacterial regrowth
293 were observed. In contrast, Aslani et al., (2014) demonstrated effective raw WW disinfection
294 by using Cu(II)/H_2O_2. In this work, the CuO/PDS system was applied to disinfect raw influent
295 of an urban WWTP. As expected, the initial pathogens abundances were much higher than those
296 in effluent: 7.3 ± 0.3 $\log_{10}$ MPN/100 mL for *E. coli*, 6.9 ± 0.3 $\log_{10}$ MPN/100 mL for
297 *Enterococcus*, and 5.5 ± 0.6 $\log_{10}$ PFU/100 mL for *F-specific RNA bacteriophages*. In contrast,
298 *spores of sulfite-reducing bacteria* were similar, with a value of 3.3 ± 0.7 $\log_{10}$ CFU/100 mL.
299 The abundances of these indicators are consistent with those found in the literature (Haramoto
300 et al., 2015; Jofre et al., 2021). Different PDS concentrations were applied to the system to
301 evaluate the influence of this parameter on the disinfection efficiency and results are shown in
302 Fig.4 (a)-(d). The CuO/PDS system was not able to eliminate *spores of sulfite-reducing bacteria*
303 at any PDS concentration (Fig. 4 (d)). The removal efficiency of *E. coli*, *Enterococcus*, and *F-*
304 *specific RNA bacteriophages* highly increased when increasing PDS concentration from 1 mM
305 to 2.5 mM, but no further significant enhancement was noticed with 10 mM PDS (Fig. 4 (a)-
306 (c)). Significant reductions of 3.5 log of *E. coli* and 4.1 log of *Enterococcus* were only reached
307 after 120 min treatment while the CuO/PDS system exhibited much better efficiency in

308 removing viruses, a 3.5 log reduction of *F-specific RNA bacteriophages* being obtained after
309 30 min treatment when using 2.5 mM PDS. This result might be related to the generation of
310 highly selective reactive species in the CuO/PDS system (see section 3.2) which have not been
311 inhibited by the very high carbon content (COD of 657 ± 55 mg/L vs 32.4 ± 5 mg/L in effluent).
312

313 **3.2. Identification of reactive species**

314 From our previous work, it was known that singlet oxygen, Cu(I) and Cu(III) are generated in
315 the CuO/PDS system (Li et al., 2021). The involvement of singlet oxygen is often questionable
316 because this latter species is quickly quenched by water. Consequently, the main aim was to
317 confirm that copper species were the main reactive species involved in disinfection processes.
318 For this purpose, the reactivity of selected nucleobases (i.e., guanine, adenosine and thymine)
319 and that of the tyrosine amino acid, a phenolic compound which was anticipated to react with
320 Cu(III) have been investigated. Degradation of ranitidine was also studied to investigate the
321 reactivity of the disulfide bridge, which is an important component of the secondary and tertiary
322 structure of proteins. This work included kinetic studies as well as the identification of
323 transformation products (TPs) by LC-HRMS. At neutral pH, no target compound was absorbed
324 on CuO (Fig. S2). As shown in Fig. 5 (a), only guanine, L-tyrosine, and ranitidine can be
325 degraded in the CuO/PDS system. Degradation kinetics of guanine and L-tyrosine fitted well
326 to the first-order kinetic model. However, guanine reacted much faster than L-tyrosine with
327 apparent kinetics rate constants k_{obs} = 0.12 ± 0.01, and 0.003 ± 0.0002 min^{-1}, respectively. In
328 contrast, the degradation kinetics of ranitidine was not a first-order kinetic since the degradation
329 stopped after 15 min. This was due to the direct reaction of ranitidine with PDS (Fig. S2)
330 resulting in a quick PDS exhaustion. Methanol (100 mM) was added as a radicals scavenger
331 (e.g., $^{\cdot}OH$ and $SO_4^{\cdot-}$). As shown in Fig 5. (b), methanol showed no inhibitory effect on the
332 guanine and ranitidine degradation and minor inhibitory effect on L-tyrosine degradation (k_{obs}

= 0.002 ± 0.0002 min^{-1}), indicating that radicals were not the predominant reactive species. This confirms the results of our previous study where singlet oxygen and Cu(III) were identified as the predominant oxidative species in the CuO/PDS system (Li et al., 2021), superoxide radical was produced from PDS decomposition, but mainly used to reduce Cu(II) to Cu(I) which contributes to the microbiocidal action of Cu(II).

To be able to discriminate between $^1O_2$ and Cu(III) contributions, TPs of guanine, L-tyrosine, and ranitidine were identified following a suspect screening workflow in LC-HRMS. For this purpose, a database was made up of a list of possible TPs with their molecular formula, exact mass, and structure (Table S4, S5, and S6). This list was established from a literature search of TPs. TPs with intensities lower than 1 $x10^4$ cps, signal to noise ratios lower than 10, isotopic ratio higher than 10%, and mass accuracy errors higher than 5 ppm were discarded. The transformation pathways of guanine (GUA), L-tyrosine (TYR), and ranitidine (RAN) were also tentatively elucidated (Fig. 6). For guanine, two main TPs were detected (Fig. S3): GUA 1 (m/z = 153.0407) and GUA 2 (m/z = 133.0243). The first step of the reaction involved a deamination reaction more likely through a one-electron oxidation process and through nitrosation of its primary amine leading to the formation of xanthine (GUA 1) followed by pyrimidine and imidazole rings opening (GUA 2). Guanine susceptibly reacts with $^1O_2$ compared with other nucleobases (Di Mascio et al., 2019). However, 8-oxoguanine, a typical TP upon $^1O_2$ reactivity was not detected supporting the predominant implication of Cu(III). Guanine was the only targeted nucleobase which was degraded because guanine has the lowest redox potential (E° = 0.81 V) among nucleobases facilitating one-electron oxidation reactions (Wang et al., 2020a; Xie et al., 2007). Similar to phenol (Li et al., 2021), L-tyrosine could be selectively oxidized by Cu(III) to generate a phenoxy radical followed by tyrosine dimerization (TYR 1 (m/z = 361.1394) and tyrosine trimerization (TYR 2 (m/z = 540.1976)) through a one-electron oxidation process (Fig. S4 and Fig. 6 (b)). Compounds corresponding to a higher degree of

polymerization could not be detected more likely due to their precipitation in the reactive medium. As shown in Fig. S5 and Fig. 6 (c), three main TPs of ranitidine were detected: RAN 1 (m/z = 331.1434), RAN 2 (m/z = 301.1279), and RAN 3 (m/z = 300.1326). RAN 1 resulted from the addition of one oxygen atom and was assigned the structure of ranitidine sulfoxide and not that of ranitidine N-oxide after injection of ranitidine N-oxide and ranitidine sulfoxide standards (Fig S6). The formation of ranitidine sulfoxide could be ascribed to the reactivity of PDS (Fig. 6). However, the contribution of Cu(III) could not be fully discarded as its formation was previously reported in presence of diperiodatocuprate (III), a stable complex of Cu(III) known as a versatile one-electron oxidant for various organic compounds (Veeresh et al., 2008). Consequently, the oxidation of other sulfur-containing compounds, such as the methionine amino acid can be anticipated in the CuO/PDS system. Simultaneously to the S oxidation reaction ranitidine could undergo an N-dealkylation reaction (RAN 2) and further transformation at the nitro moiety leading to RAN 3 (tentative structure).

In summary, Cu(III) was found to be the predominant reactive species generated in the CuO/PDS system with extremely fast and selective reactivity with guanine which can lead to DNA damages. This result supports the higher efficiency of the CuO/PDS system in eliminating non-enveloped viruses (e.g., bacteriophages) in raw WW with respect to bacteria and the lack of bacterial regrowth. However, the CuO/PDS system can also selectively oxidize disulfide bridge and phenolic amino acids with a strong impact on proteins and enzyme integrity also facilitating pathogens inactivation.

3.3 Antibiotic-resistant bacteria and antibiotic resistance genes (ARB&Gs) removal

SMX (516 mg/L), as one of the first antibiotics for which bacterial resistance was observed (Pazda et al., 2019), was spiked to the culture medium to study the SMX-resistant bacteria. The initial concentration of SMX-resistant *E. coli* was 4.7 $\log_{10}$ CFU/100 mL (Fig. 7 (a)) and the

prevalence was 15.8% (Fig. 7 (b)). SMX-resistant *Enterococcus* was not detected, which suggests that no *Enterococcus* was cultivable under this SMX concentration level. A significant reduction of SMX-resistant *E. coli* (3.2 log) was observed after 10 min of treatment (Fig. 7 (a)). In addition, further abatement of SMX- resistant *E. coli* was also observed during storage time in untreated and treated WW samples (Fig. 7 (a)), however, the prevalence of SMX-resistant *E. coli* in untreated WW samples was even increased up to 38.5% after 24 h storage (Fig. 7 (b)), which indicated that the reduction of SMX-resistant *E. coli* was slower than that of total *E.* coli. Consequently, the CuO/PDS system presented an excellent inactivation effect on SMX-resistant *E. coli* and could also effectively prevent from the enrichment of SMX-resistant bacteria.

The abundances reduction of ARGs was also evaluated. Antibiotic resistance spreads through getting resistance genes, which exist in their core genome or on mobile genetic elements, such as transposons, integrons, and plasmids (Babakhani and Oloomi, 2018). Therefore, the resistance genes (blaTEM, qrnS, emrB, and sul1) for the most commonly used groups of antibiotics (beta-lactams, quinolones, macrolides, and sulfonamides, respectively) were selected. Class 1 integron-integrase gene (intI1), and the IS613 insertion sequence were also investigated. In addition to these, 16S rRNA gene was selected as a biomarker for bacteria, aiming at assessing the reduction in the load of total bacteria.

The mean values of initial abundances of examined genes were 3.1, 3.8, 4.3, 4.8, 4.9, 4.6, and 7.0 $\log_{10}$ (N copies/mL) of blaTEM, qrnS, emrB, sul1, intI1, IS613, and 16S rRNA, respectively (Fig. 8 (a)), and these values are similar to those reported in urban WWTP effluents by Wang et al., (2020b) for instance. An average reduction of 1.0 log blaTEM (90% abatement), 0.7 log qrnS (81% abatement), 0.9 log emrB (87% abatement), 1.0 log sul1(90% abatement), 2.3 log intI1 (99% abatement), 0.8 log IS613 (83% abatement), and 0.6 log 16SrRNA (90% abatement) was achieved after 60 min treatment (Fig. 8 (a)), which is as effective as chlorination and UV irradiation, which caused 1.04-2.45 log and 0.59-0.96 log reduction of blaTEM and 2.98-3.14

log and 2.48-2.74 log reduction of intI1 (Phattarapattamawong et al., 2021; Sharma et al., 2016). It is also noted that the reduction of pathogens and resistant *E. coli* by the system was much effective than the reduction of 16S rRNA gene. This was probably due to the Cu(III) reactivity that led to the induction of a 'Viable But Not Cultivable state' (VBNC) of bacteria and non-cultivable bacteria were detectable using the 16S rRNA measurement approach. In addition, chlorination, UV irradiation, and ozone treatments have been investigated to remove ARGs, but usually it is necessary to increase the disinfectant or UV doses and contact time to achieve a significant reduction in ARGs (Chen et al., 2020; Iakovides et al., 2019; Phattarapattamawong et al., 2021; Sharma et al., 2016; Yuan et al., 2015). The presence of the targeted genes within the total microbial community was estimated by using the relative abundances of ARGs, which were normalized to the 16S rRNA gene copy number. Results are expressed in the logarithmic scale and shown in Fig. 8 (b), where values of -2, -3, and -4 indicate the presence of one resistance gene for every 100, 1000, and 10000 copies of 16S rRNA gene, respectively. The initial relative abundances of targeted genes varied from -3.85 ± 0.1 log of blaTEM to -2.08 ± 0.1 log of intI1 and the rank of abundances was determined as intI1 > sul1 > IS613 > ermB > qnrS > blaTEM in WW, while the rank of abundances in treated WW was determined as IS613 (-2.5 ± 0.2 log) > sul1 > ermB > qnrS > intI1 > blaTEM (-4.3 ± 0.3 log). The relative abundances reduction was observed for all targeted genes, especially for intI1, which indicated that the spread of ARGs was effectively limited by using the CuO/PDS system. Optimizing operational conditions such as longer contact time and/or the use of higher doses of CuO should improve the removal rates of targeted ARGs but this was outside the scope of this work.

4. Conclusions

Studies on the disinfection of raw and secondary treated WW demonstrated that CuO/PDS system was an effective disinfection technology in comparison to CuO alone, and sulfate

radical-based system. Chlorination was probably more effective but the CuO/PDS had the advantage to avoid the production of halogenated DBPs in organic-rich WW. This work also revealed that Cu(III) instead of singlet oxygen might be the major reactive species responsible for pathogens inactivation. Due to the high selectivity of Cu(III), disinfection was still effective in raw WW as this latter oxidative species was not inhibited by the high content in organic matter. This was particularly true against viruses because of the very fast and selective reactivity of Cu(III) against guanine, possibly causing high DNA damages and avoiding bacterial regrowth after treatment. In addition, the effective reduction of selected ARB&Gs by CuO/PDS system was demonstrated by using SMX-resistant *E. coli* as a probe for ARBs, and blaTEM, qrnS, emrB, sul1, intI, and IS613 as selected ARGs. Collectively, all these findings led us to conclude that the CuO/PDS system might be a promising disinfection technology for WW treatment and reuse in irrigation mainly because it is effective in removing a large range of pathogens while preserving the carbon and nutrients content of WW and because it might be easily implemented at field-scale through filtration units. Nevertheless, this study was carried out in beakers, which is not a good option to achieve the recycling of CuO microparticles. To overcome this shortcoming, a fixed-bed column packed with CuO has been set up by our research group for investigating wastewater disinfection, as well as wastewater decontamination. Also, economic analysis and risk assessment are needed to be made based on the fixed-bed column in terms of PDS consumption and CuO stability. These efforts will contribute to improving the feasibility of the CuO/PDS system in future water remediation applications.

Acknowledgements: This research was financially supported by the Water Joint Programming Initiative (JPI) through the research project IDOUM - Innovative Decentralized and low cost treatment systems for Optimal Urban wastewater Management. Chan Li thanks the Occitanie

Region for her PhD grant.

References

Akhoundi, A., Nazif, S., 2018. Sustainability assessment of wastewater reuse alternatives using the evidential reasoning approach. J. Clean. Prod. 195, 1350–1376. https://doi.org/10.1016/j.jclepro.2018.05.220

Aslani, H., Nabizadeh, R., Alimohammadi, M., Mesdaghinia, A., Nadafi, K., Nemati, R., Ghani, M., 2014. Disinfection of raw wastewater and activated sludge effluent using Fenton like reagent. J. Environ. Heal. Sci. Eng. 12, 1–7. https://doi.org/10.1186/s40201-014-0149-8

Babakhani, S., Oloomi, M., 2018. Transposons: the agents of antibiotic resistance in bacteria. J. Basic Microbiol. 58, 905–917. https://doi.org/10.1002/jobm.201800204

Chen, L., Zhou, Z., Shen, C., Xu, Y., 2020. Inactivation of antibiotic-resistant bacteria and antibiotic resistance genes by electrochemical oxidation/electroFenton process. Water Sci. Technol. 81, 2221–2231. https://doi.org/10.2166/wst.2020.282

Chen, Y. di, Duan, X., Zhou, X., Wang, R., Wang, S., Ren, N. qi, Ho, S.H., 2021. Advanced oxidation processes for water disinfection: Features, mechanisms and prospects. Chem. Eng. J. 409, 128207. https://doi.org/10.1016/j.cej.2020.128207

Cho, Y.C., Lin, R.Y., Lin, Y.P., 2020. Degradation of 2,4-dichlorophenol by CuO-activated peroxydisulfate: Importance of surface-bound radicals and reaction kinetics. Sci. Total Environ. 699, 134379. https://doi.org/10.1016/j.scitotenv.2019.134379

CLSI, 2020. CLSI M100: Performance Standards for Antimicrobial Susceptibility Testing , 29th Edition, Clsi.

Collivignarelli, M.C., Abbà, A., Benigna, I., Sorlini, S., Torretta, V., 2018. Overview of the main disinfection processes for wastewater and drinking water treatment plants. Sustain. 10, 1–21. https://doi.org/10.3390/su10010086

de la Obra Jiménez, I., Giannakis, S., Grandjean, D., Breider, F., Grunauer, G., Casas López, J.L., Sánchez Pérez, J.A., Pulgarin, C., 2020. Unfolding the action mode of light and

484 homogeneous vs. heterogeneous photo-Fenton in bacteria disinfection and concurrent
485 elimination of micropollutants in urban wastewater, mediated by iron oxides in Raceway
486 Pond Reactors. Appl. Catal. B Environ. 263, 118158.
487 https://doi.org/10.1016/j.apcatb.2019.118158
488 de Melo Costa-Serge, N., Gonçalves, R., Rojas-Mantilla, H., Santilli, C., Hammer, P., Pupo
489 Nogueira, R., 2021. Fenton-like degradation of sulfathiazole using copper-modified
490 MgFe-CO3 layered double hydroxide. J. Hazard. Mater. 413, 125388.
491 https://doi.org/10.1016/j.jhazmat.2021.125388
492 Di Mascio, P., Martinez, G.R., Miyamoto, S., Ronsein, G.E., Medeiros, M.H.G., Cadet, J., 2019.
493 Singlet molecular oxygen reactions with nucleic acids, lipids, and proteins. Chem. Rev.
494 119, 2043–2086. https://doi.org/10.1021/acs.chemrev.8b00554
495 Dias, E., Ebdon, J., Taylor, H., 2018. The application of bacteriophages as novel indicators of
496 viral pathogens in wastewater treatment systems. Water Res. 129, 172–179.
497 https://doi.org/10.1016/j.watres.2017.11.022
498 Dizaj, S.M., Lotfipou, F., Barzegar-jalali, M., Zarrintan Hossein, M., Adibkia, K., 2014.
499 Antimicrobial activity of the metals and metal oxide nanoparticles. Mater. Sci. Eng. C 44,
500 278–284. https://doi.org/10.1016/j.msec.2014.08.031
501 EU, 2020. Official Journal of the European Union. Off. J. Eur. Union.
502 García-Fresnadillo, D., 2018. Singlet oxygen photosensitizing materials for point-of-use water
503 disinfection with solar reactors. ChemPhotoChem, 2(7), 512-534.
504 https://doi.org/10.1002/cptc.201800062
505 Gehr, R., Wagner, M., Veerasubramanian, P., Payment, P., 2003. Disinfection efficiency of
506 peracetic acid, UV and ozone after enhanced primary treatment of municipal wastewater.
507 Water Res. 37, 4573–4586.https://doi.org/10.1016/S0043-1354(03)00394-4
508 Ghulam, M., Hajira, T., Muhammad, S., Nasir, A., 2013. Synthesis and characterization of

509 cupric oxide (CuO) nanoparticles and their application for the removal of dyes. African
510 J. Biotechnol. 12, 6650–6660. https://doi.org/10.5897/ajb2013.13058
511 Haramoto, E., Fujino, S., Otagiri, M., 2015. Distinct behaviors of infectious F-specific RNA
512 coliphage genogroups at a wastewater treatment plant. Sci. Total Environ. 520, 32–38.
513 https://doi.org/10.1016/j.scitotenv.2015.03.034
514 Hashemi, H., Bovini, A., Hung, Y., Amin, M., 2013. A review on wastewater disinfection. Int.
515 J. Environ. Health Eng. 2, 22. https://doi.org/10.4103/2277-9183.113209
516 Hong, P.Y., Al-Jassim, N., Ansari, M.I., Mackie, R.I., 2013. Environmental and public health
517 implications of water reuse: Antibiotics, antibiotic resistant bacteria, and antibiotic
518 resistance genes. Antibiotics. https://doi.org/10.3390/antibiotics2030367
519 Hong, P.Y., Julian, T.R., Pype, M.L., Jiang, S.C., Nelson, K.L., Graham, D., Pruden, A., Manaia,
520 C.M., 2018. Reusing treated wastewater: Consideration of the safety aspects associated
521 with antibiotic-resistant bacteria and antibiotic resistance genes. Water (Switzerland) 10.
522 https://doi.org/10.3390/w10030244
523 Hwangbo, M., Claycomb, E.C., Liu, Y., Alivio, T.E.G., Banerjee, S., Chu, K.H., 2019.
524 Effectiveness of zinc oxide-assisted photocatalysis for concerned constituents in reclaimed
525 wastewater: 1,4-Dioxane, trihalomethanes, antibiotics, antibiotic resistant bacteria (ARB),
526 and antibiotic resistance genes (ARGs). Sci. Total Environ. 649, 1189–1197.
527 https://doi.org/10.1016/j.scitotenv.2018.08.360
528 Iakovides, I.C., Michael-Kordatou, I., Moreira, N.F.F., Ribeiro, A.R., Fernandes, T., Pereira,
529 M.F.R., Nunes, O.C., Manaia, C.M., Silva, A.M.T., Fatta-Kassinos, D., 2019. Continuous
530 ozonation of urban wastewater: Removal of antibiotics, antibiotic-resistant Escherichia
531 coli and antibiotic resistance genes and phytotoxicity. Water Res. 159, 333–347.
532 https://doi.org/10.1016/j.watres.2019.05.025
533 Jaramillo, M.F., Restrepo, I., 2017. Wastewater reuse in agriculture: A review about its

limitations and benefits. Sustain. https://doi.org/10.3390/su9101734

Jofre, J., Lucena, F., Blanch, A.R., 2021. Bacteriophages as a complementary tool to improve the management of urban wastewater treatments and minimize health risks in receiving waters. Water (Switzerland) 13. https://doi.org/10.3390/w13081110

Karkman, A., Do, T.T., Walsh, F., Virta, M.P.J., 2018. Antibiotic-resistance genes in waste water. Trends Microbiol. 26, 220–228. https://doi.org/10.1016/j.tim.2017.09.005

Kim, H.E., Nguyen, T.T.M.M., Lee, H., Lee, C., 2015. Enhanced inactivation of Escherichia coli and MS2 coliphage by cupric ion in the presence of hydroxylamine: Dual microbicidal effects. Environ. Sci. Technol. 49, 14416–14423. https://doi.org/10.1021/acs.est.5b04310

Kitis, M., 2004. Disinfection of wastewater with peracetic acid: A review. Environ. Int. 30, 47–55. https://doi.org/10.1016/S0160-4120(03)00147-8

Li, C., Goetz, V., Chiron, S., 2021. Peroxydisulfate activation process on copper oxide: Cu(III) as the predominant selective intermediate oxidant for phenol and waterborne antibiotics removal. J. Environ. Chem. Eng. 9, 105145. https://doi.org/10.1016/j.jece.2021.105145

Lu, S., Liu, L., Demissie, H., An, G., Wang, D., 2021 Design and application of metal-organic frameworks and derivatives as heterogeneous Fenton-like catalysts for organic wastewater treatment: A review. Environ. Intern. 146, 106273. https://doi.org/10.1016/j.envint.2020.106273

Mandilara, G.D., Smeti, E.M., Mavridou, A.T., Lambiri, M.P., Vatopoulos, A.C., Rigas, F.P., 2006. Correlation between bacterial indicators and bacteriophages in sewage and sludge. FEMS Microbiol. Lett. 263, 119–126. https://doi.org/10.1111/j.1574-6968.2006.00414.x

Núñez-Salas, R.E., Rodríguez-Chueca, J., Hernández-Ramírez, A., Rodríguez, E., Maya-Treviño, M.D.L., 2021. Evaluation of B-ZnO on photocatalytic inactivation of Escherichia coli and Enterococcus sp. J. Environ. Chem. Eng. 9. https://doi.org/10.1016/j.jece.2020.104940

559 Odonkor, S.T., Ampofo, J.K., 2013. Escherichia coli as an indicator of bacteriological quality
560 of water: an overview. Microbiol. Res. (Pavia). 4, 2. https://doi.org/10.4081/mr.2013.e2
561 Pazda, M., Kumirska, J., Stepnowski, P., Mulkiewicz, E., 2019. Antibiotic resistance genes
562 identified in wastewater treatment plant systems – A review. Sci. Total Environ. 697,
563 134023. https://doi.org/10.1016/j.scitotenv.2019.134023
564 Phattarapattamawong, S., Chareewan, N., Polprasert, C., 2021. Comparative removal of two
565 antibiotic resistant bacteria and genes by the simultaneous use of chlorine and UV
566 irradiation (UV/chlorine): Influence of free radicals on gene degradation. Sci. Total
567 Environ. 755, 142696. https://doi.org/10.1016/j.scitotenv.2020.142696
568 Sánchez-Ruiz, C., Martínez-Royano, S., & Tejero-Monzón, I. (1995). An evaluation of the
569 efficiency and impact of raw wastewater disinfection with peracetic acid prior to ocean
570 discharge. Water Sci. and Technol., 32(7), 159-166.
571 Sharma, V.K., Johnson, N., Cizmas, L., McDonald, T.J., Kim, H., 2016. A review of the
572 influence of treatment strategies on antibiotic resistant bacteria and antibiotic resistance
573 genes. Chemosphere 150, 702–714. https://doi.org/10.1016/j.chemosphere.2015.12.084
574 Vasilyak, L.M., 2021. Physical Methods of Disinfection (A Review). Plasma Phys. Reports 47,
575 318–327. https://doi.org/10.1134/S1063780X21030107
576 Veeresh, T.M., Patil, R.K., Nandibewoor, S.T., 2008. Thermodynamic quantities for the
577 oxidation of ranitidine by diperiodatocuprate(III) in aqueous alkaline medium. Transit.
578 Met. Chem. 33, 981–988. https://doi.org/10.1007/s11243-008-9140-5
579 W.H. Organization, 2015. Global Antimicrobial Resistance Surveillance System.
580 http://apps.who.int/iris/bitstream/10665/188783/1/9789241549400_eng.pdf?ua=1.
581 Wang, J., Chu, L., Wojnárovits, L., Takács, E., 2020b. Occurrence and fate of antibiotics,
582 antibiotic resistant genes (ARGs) and antibiotic resistant bacteria (ARB) in municipal
583 wastewater treatment plant: An overview. Sci. Total Environ. 744, 140997.

https://doi.org/10.1016/j.scitotenv.2020.140997

Wang, J., Yang, S., Zhang, Y., 2020a. One-electron oxidation and redox potential of nucleobases and deoxyribonucleosides computed by QM/MM simulations. Chem. Phys. Lett. 739, 136948. https://doi.org/10.1016/j.cplett.2019.136948

Xia, D., Li, Y., Huang, G., Yin, R., An, T., Li, G., Zhao, H., Lu, A., Wong, P.K., 2017. Activation of persulfates by natural magnetic pyrrhotite for water disinfection: Efficiency, mechanisms, and stability. Water Res. 112, 236–247. https://doi.org/10.1016/j.watres.2017.01.052

Xie, H., Yang, D., Heller, A., Gao, Z., 2007. Electrocatalytic oxidation of guanine, guanosine, and guanosine monophosphate. Biophys. J. 92, 70–72. https://doi.org/10.1529/biophysj.106.102632

Yuan, Q. Bin, Guo, M.T., Yang, J., 2015. Fate of antibiotic resistant bacteria and genes during wastewater chlorination: Implication for antibiotic resistance control. PLoS One 10, 1–11. https://doi.org/10.1371/journal.pone.0119403

Zhang, T., Chen, Y., Wang, Y., Le Roux, J., Yang, Y., Croué, J.P., 2014. Efficient peroxydisulfate activation process not relying on sulfate radical generation for water pollutant degradation. Environ. Sci. Technol. 48, 5868–5875. https://doi.org/10.1021/es501218f

Figure captions

Fig. 1. Inactivation profiles of pathogens: (a) E. Coli, (b) Enterococcus, (c) F-specific RNA bacteriophages and (d) spore of sulfite-reducing bacteria by different disinfection systems: CuO, PDS, CuO/PDS, thermally activated persulfate ($SO_4^{\cdot-}$) and chlorination (Cl_2). [CuO]= 10 g/L, [PDS]= 1 mM, secondary treated wastewater. Note: the unshown rectangles from 15 min to 120 min represent that the concentrations of pathogens were lower than the limit of detection (LOD).

Fig. 2. Concentration of (a) leached Cu(II) and (b) PDS during CuO/PDS treatment of secondary treated wastewater. [CuO] = 10 g/L, [PDS] = 1 mM.

Fig. 3. Regrowth profiles of E. Coli and Enterococcus in secondary treated wastewater after (a) 5 min and (b) 10 min CuO/PDS treatment. [CuO] = 10 g/L, [PDS] = 1 mM.

Fig. 4. Inactivation profiles of pathogens in raw wastewater using CuO/PDS system and different PDS concentrations: (a) E. Coli, (b) Enterococcus, (c) F-specific RNA bacteriophages and (d) spores of sulfite-reducing bacteria. [CuO] = 10 g/L, [PDS] = 1, 2.5, 10 mM Note: NM = not measured.

Fig 5. Degradation kinetics of (a) targeted compounds, and (b) the effect of methanol in distilled water using the CuO/PDS system. [CuO] = 10 g/L, [PDS] = 1 mM, [adenosine] = [thymine] = [guanine] = [ranitidine] = [L-tyrosine] = 20 mg/L, [methanol] = 100 mM at pH = 7 (Tris buffer).

Fig. 6. Proposed transformation pathways of (a) guanine (GUA), (b) L-tyrosine (TYR), and (c) ranitidine (RAN) in CuO/PDS system.

Fig. 7. Inactivation profiles of SMX-resistant E. Coli after 10 min treatment by CuO/PDS systems in secondary treated wastewater. [CuO] = 10 g/L, [PDS] = 1 mM. Note: the unshown rectangles after treatment mean that the concentrations were lower than the limits of detection of methods.

Fig. 8. Reduction profiles of selected ARGs after 60 min treatment by CuO/PDS system in secondary treated wastewater, expressed as (a) mean value and (b) relative abundances of ARGs normalized to 16S r RNA. [CuO] = 10 g/L, [PDS] = 1 mM.

Table captions

Table 1. Major physico-chemical properties of the investigated urban wastewater.

Table 2. Concentration (µg/L) of chloroform (CFL), dichloromonobromomethane (DCB), monochlorodibromomethane (MCB), bromoform (BRF) and total trihalomethanes (THMs) formed in different disinfection systems after 120 min of treatment.

Table 1

Parameter	Influent	Effluent
EC (mS/cm)	2.1 ± 0.5	1.6 ± 0.4
pH	7.5 ± 0.1	7.7 ± 0.1
TSS (mg/L)	115 ± 32	8.2 ± 2.6
COD (mg/L)	657 ± 55	32.4 ± 5
HCO_3^- (mg/L)	n.d	514.3
Cl^- (mg/L)	n.d	195.3
NO_3^- (mg/L)	< LOD	12.9 ± 1.5
NH_4^+ (mg/L)	26 ± 5	0.5
PO_4-P (mg/L)	6.8 ± 1.2	0.6 ± 0.2
SO_4^{2-} (mg/L)	n.d	58.9
Cu (µg/L)	n.d	3.75

n.d: not determined

Table 2

DBPs (μg/L)	Cl_2	CuO	$SO_4^{\cdot-}$	CuO/PDS
CFL	30	<0.5	<0.5	<0.5
DCB	10	<0.5	<0.5	<0.5
MCB	2.7	<0.5	<0.5	<0.5
BRF	<0.5	<0.5	<0.5	<0.5
THMs	42.7	<0.5	<0.5	<0.5

Figure 1

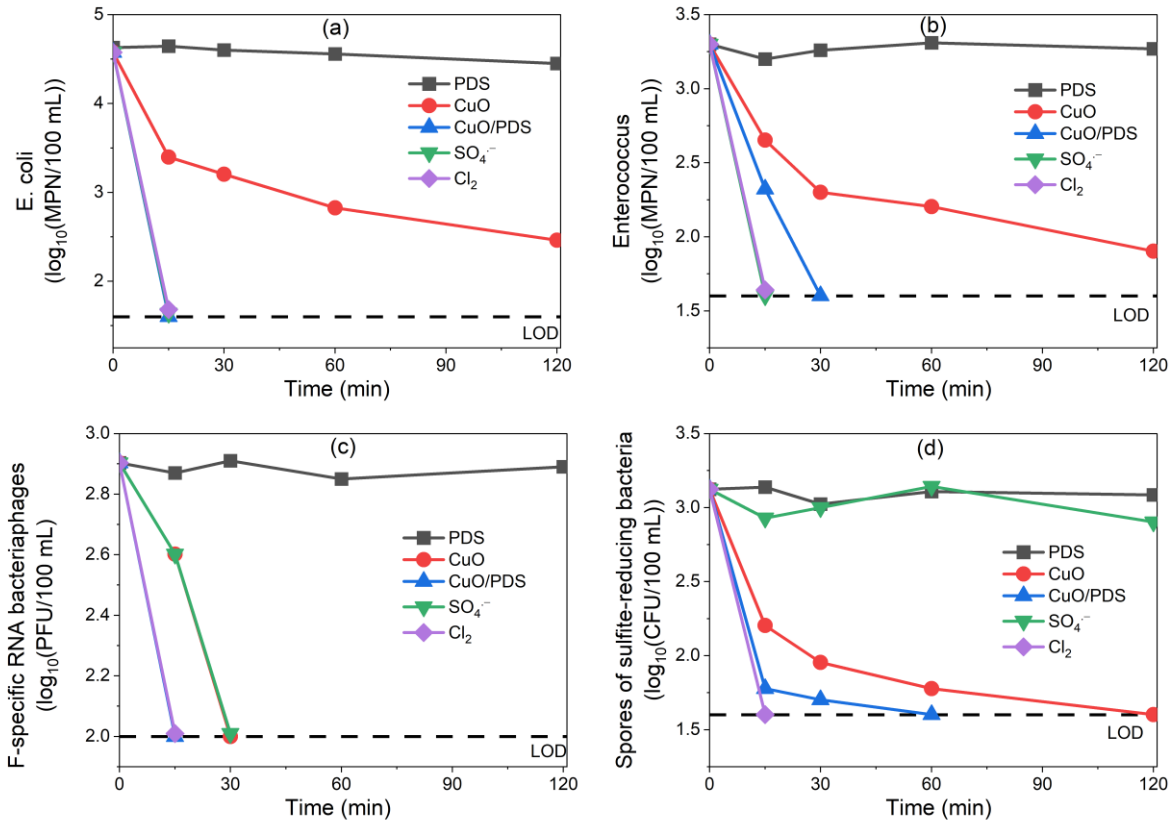

Figure 2

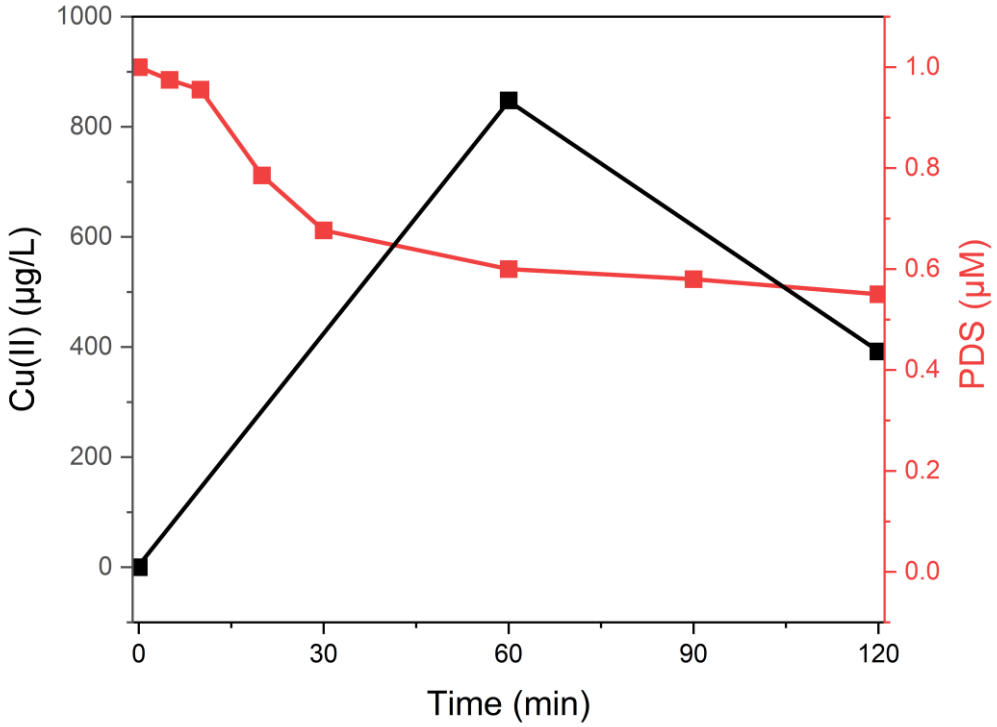

Figure 3

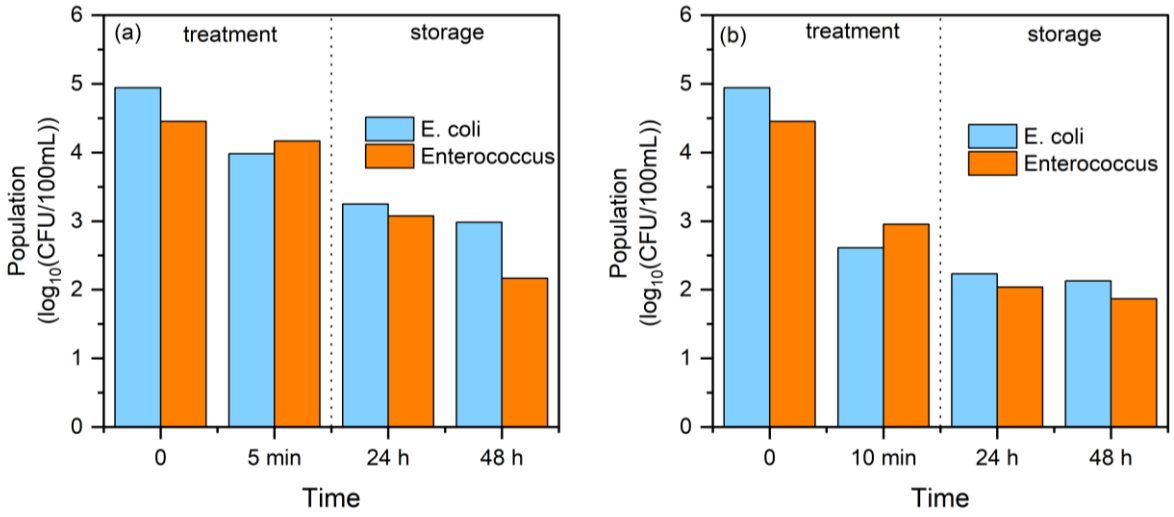

668 Figure 4

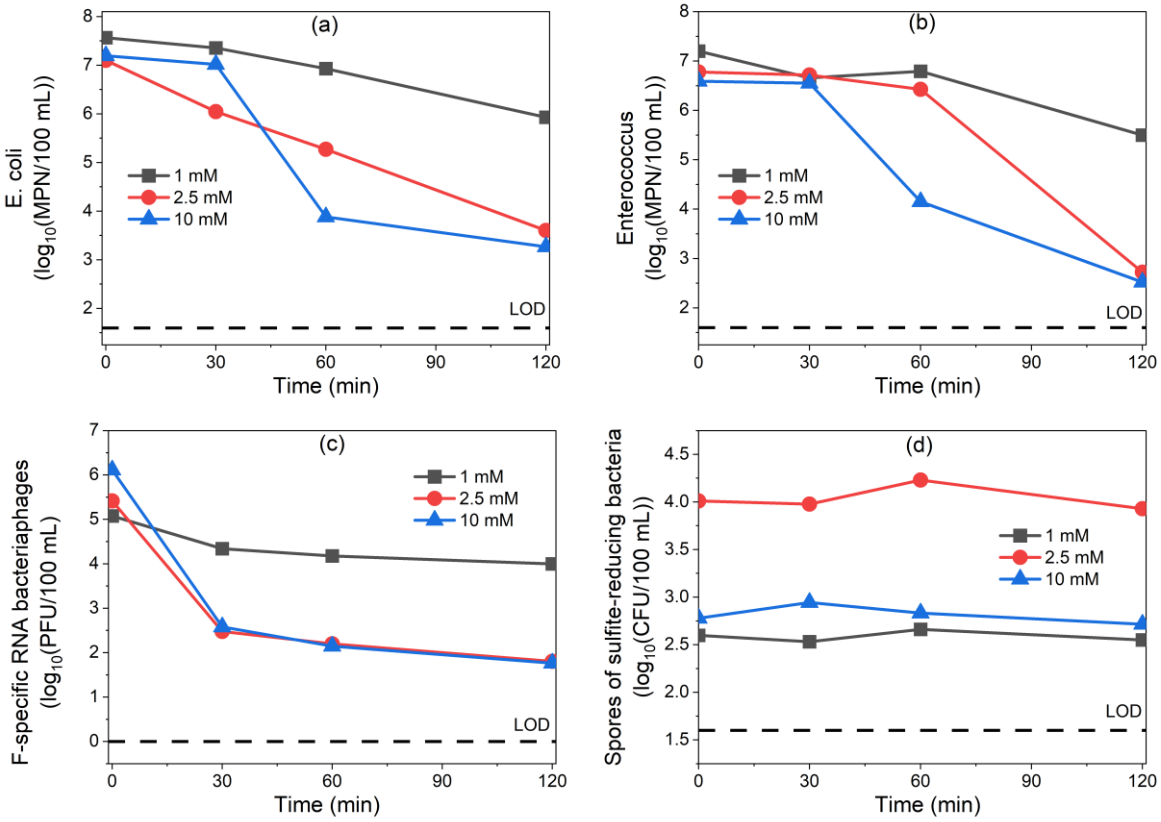

669

670

671 Figure 5

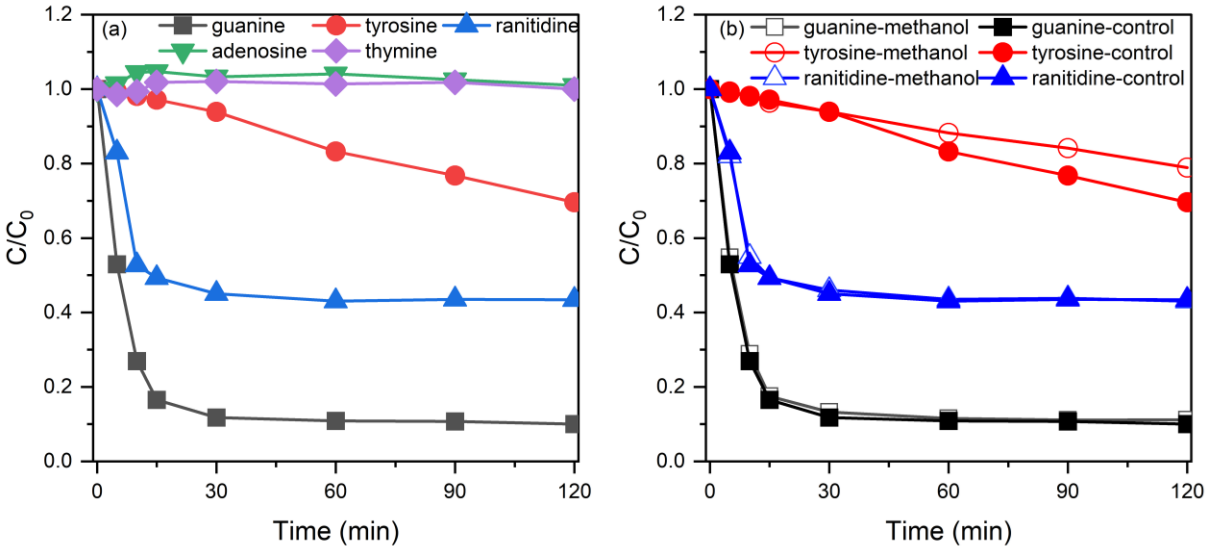

672

673

674 Figure 6

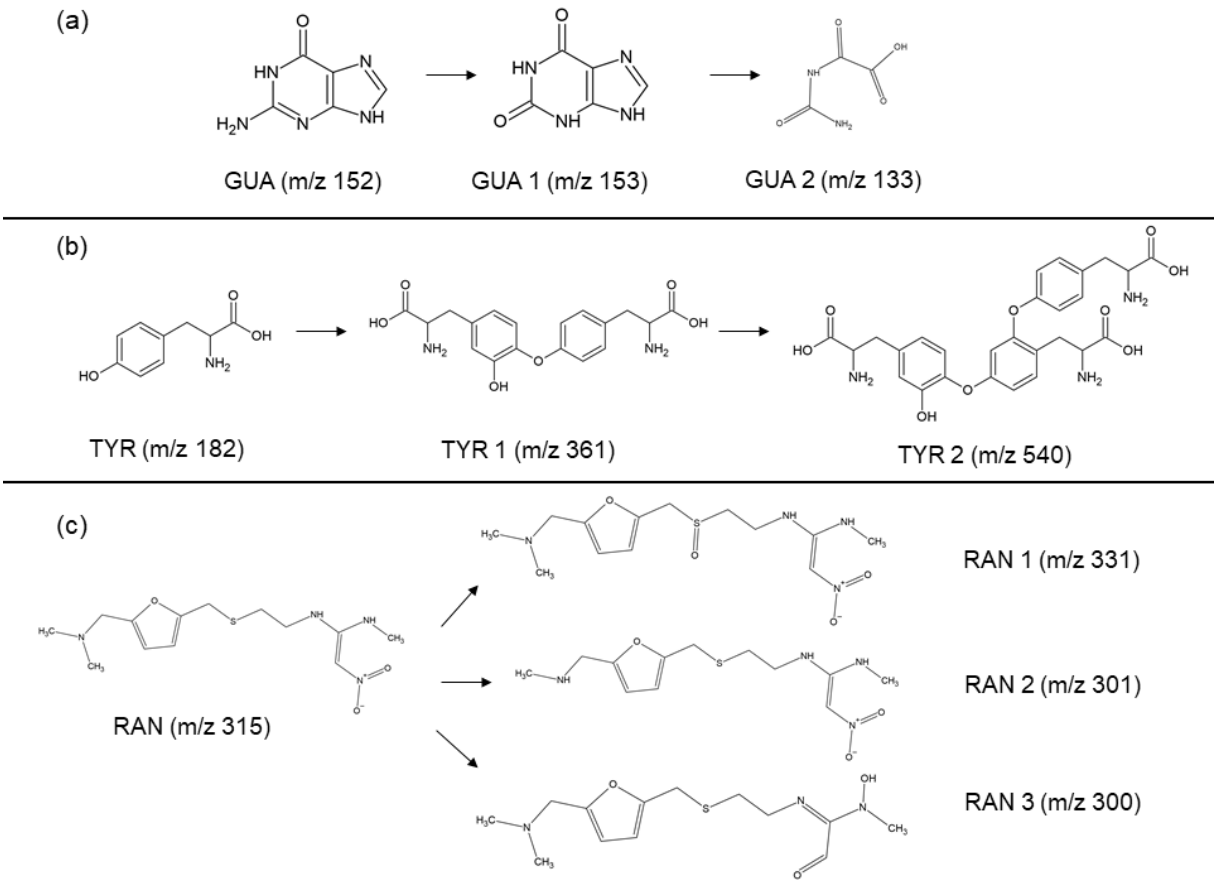

675

676

677 Figure 7

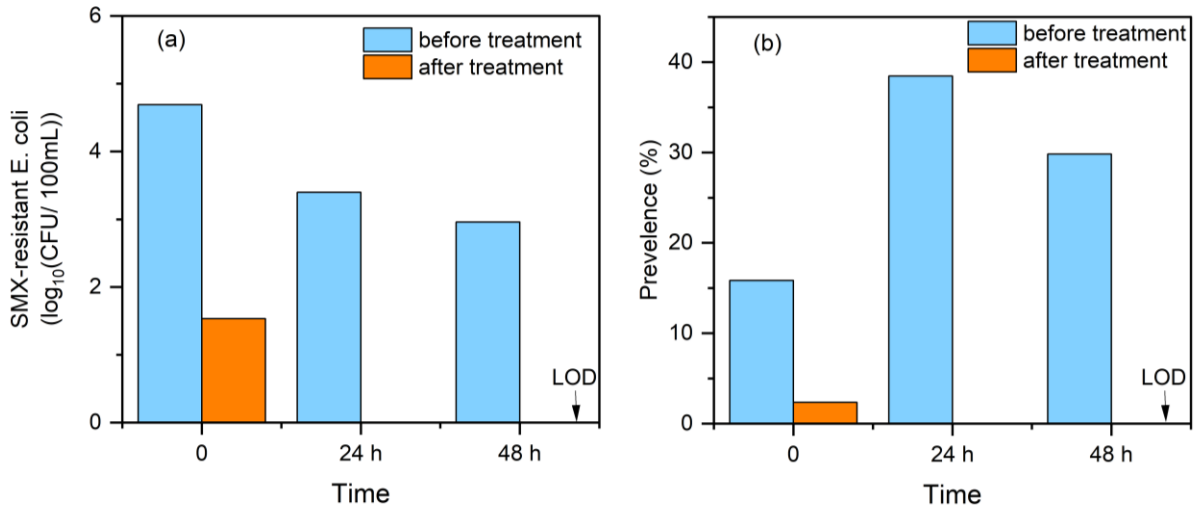

678

679 Figure 8

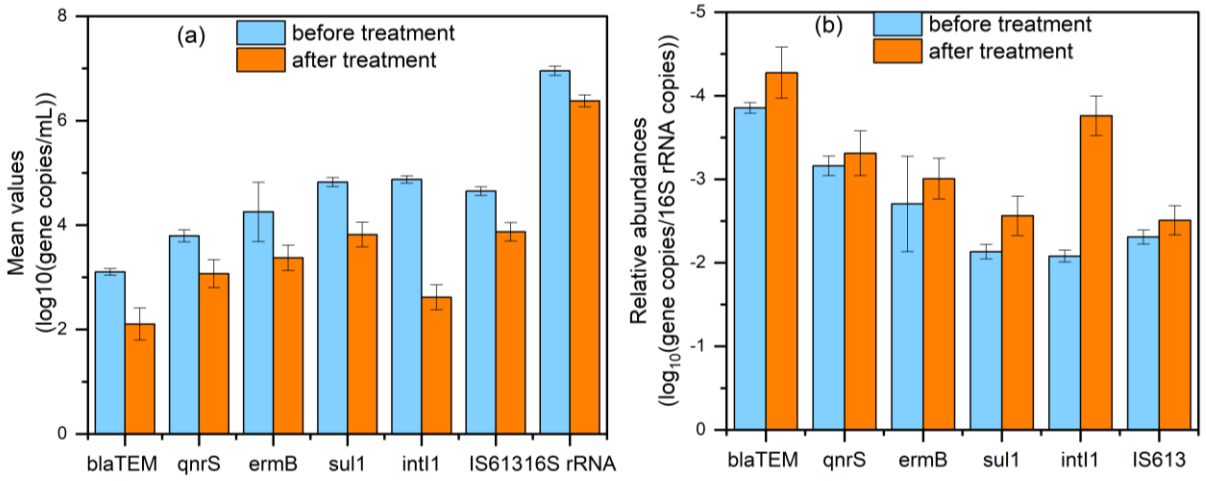

680

681